

Evidence for a logarithmic pinning barrier in $\text{Bi}_2\text{Sr}_2\text{Ca}_2\text{Cu}_3\text{O}_x$ tapes

R. Hergt, R. Hiergeist, and J. Taubert

Institut für Physikalische Hochtechnologie, Helmholtzweg 4, D-O-6900 Jena, Germany

H. W. Neumueller and G. Ries

Siemens AG, Research Laboratories, PF 3220, D-W-8520 Erlangen, Germany

(Received 1 June 1992; revised manuscript received 24 September 1992)

Relaxation measurements using torque magnetometry were performed for textured $\text{Bi}_2\text{Sr}_2\text{Ca}_2\text{Cu}_3\text{O}_x$ tapes at 77 K. Experiments were carried out for different orientations of the external field with respect to the texture axis (defined as the c axis), which coincides with the tape normal. The experimental torque data were separated into reversible and irreversible anisotropic contributions. It is shown that the irreversible contribution scales with the field component parallel to the c axis. Relaxation data investigated nearly up to equilibrium show a power-law behavior $\ln(M/M_0) \propto \ln(t/t_0)$. The results indicate a logarithmic pinning barrier $U(J) \propto \ln(J_0/J)$. The dependence of the barrier height on the field component parallel to the texture axis is determined from experiments with different orientations of external fields up to 400 kA/m. From relaxation curves, relations between the current density and the electric field are derived that obey a power law over five orders of magnitude of the induced electric field. The results are compared with electrical-transport data. Pinning potentials derived from torque as well as electrical-transport studies for different magnitude and orientation of the magnetic field scale well with the field component parallel to the c axis. The results are discussed in the framework of weakly coupled pancake vortices.

I. INTRODUCTION

A typical feature of high- T_c superconductors in comparison to conventional ones is the occurrence of giant flux-creep effects. These effects were investigated in a large number of papers by measuring magnetization relaxation. In early experiments magnetization decay currently was found to obey a logarithmic relaxation law which may be understood in the frame of the Anderson-Kim flux-creep model.¹ The logarithmic decay law of the Anderson-Kim model¹ results from the assumption of a linear dependence of the pinning barrier on current density. For long times the logarithmic decay in this model changes to an exponential approach to equilibrium. Several recent experimental observations indicate deviations from that model.²⁻⁹ Nonlogarithmic relaxation behavior was found, for instance, by Thompson, Sun, and Holtzberg³ for proton-irradiated single crystals of $\text{YBa}_2\text{Cu}_3\text{O}_7$ (Y-Ba-Cu-O) at 30 K, by Konczykowski, Malozemoff, and Holtzberg⁴ for Y-Ba-Cu-O single crystals near T_c , and by Sandvold and Rossel⁵ for Y-Ba-Cu-O films. The data are interpreted by means of an interpolation formula,² which at short times reduces to the Anderson-Kim form and in the long-time limit crosses over to a $[\ln(t)]^{-1/p}$ decay. This formula may be understood in the frame of the vortex-glass model⁶ as well as in the collective-creep model (e.g., Ref. 7). Experimentally observed deviations from the logarithmic decay law may be related to deviations of the current dependence of the barrier from the linear law of the Anderson-Kim model.¹ The interpolation formula is related to an inverse power-law barrier. A logarithmic dependence of the pinning potential on the current density was suggested by Zeldov

*et al.*⁹ for explaining relaxation data of Y-Ba-Cu-O films. The dependence of the effective pinning barrier on the magnetization (i.e., the current density) was measured by Maley and Willis¹⁰ and McHenry *et al.*¹¹ for grain-aligned Y-Ba-Cu-O as well as single crystals of $\text{La}_{1.8}\text{Sr}_{0.14}\text{CuO}_4$, respectively. They found a somewhat better fit of the experimental results assuming a logarithmic barrier rather than an inverse power law. From a theoretical point of view, Vinokur *et al.*¹² have pointed out that the logarithmic current dependence provides a good approximation for the creep activation barrier in the single-vortex creep regime. For this case an exact solution of the flux-creep problem was given by Vinokur, Feigelman, and Geshkenbein¹³ which results in self-organized criticality. A completely different approach to the flux-creep problem assumes a distribution of pinning barriers (e.g., Ref. 14). Common to all single-barrier models, deviations from a logarithmic decay law become apparent only after appreciable decay of magnetization. However, for reasons of experimental sensitivity, most investigations are performed under conditions where the effective pinning barriers are high in comparison to kT ; i.e., either the pinning centers are relatively strong as, for instance, in Y-Ba-Cu-O in comparison to Bi-Sr-Ca-Cu-O or the temperature and magnetic field are sufficiently low. For the extremely anisotropic materials of Bi-Sr-Ca-Cu-O or Tl-Ba-Ca-Cu-O type, there are a few papers in the literature which report deviations from a logarithmic relaxation law. Shi and Xu,¹⁵ for instance, interpret their nonlogarithmic relaxation data for single crystals of $\text{Bi}_2\text{Sr}_2\text{CaCu}_2\text{O}_x$ by the interpolation formula originating from the collective-creep model.⁷ Evidence for collective flux pinning is claimed by Svedlindh *et al.*¹⁶ for

$\text{Bi}_{2.2}\text{Sr}_{1.7}\text{CaCu}_2\text{O}_x$ single crystals. van der Beek *et al.*¹⁷ find for a $\text{Bi}_2\text{Sr}_2\text{CaCu}_2\text{O}_x$ single crystal a logarithmic dependence $U(J)$ with deviations at low current densities. In the framework of the collective-creep model, they describe their data by an inverse power-law barrier, the power of which varies continuously with current density. Maley *et al.*¹⁸ report for Pb-doped $\text{Bi}_2\text{Sr}_2\text{Ca}_2\text{Cu}_3\text{O}_x$ tape that their results can be fit quite well with the logarithmic form of $U(J)$.

Relaxation measurements reported in the literature mainly are confined to the case of the magnetic field being parallel to the crystal c axis. For inclined field directions peculiarities of the vortex structure occur especially in the case of clearly layered materials of the Bi-Sr-Ca-Cu-O type that have consequences for the relaxation behavior. In the present paper we combine relaxation measurements with investigations of the anisotropy of flux line pinning in Bi-Sr-Ca-Cu-O. In particular, we report relaxation data in a rapid relaxation regime for the field being inclined with respect to the c axis. We investigate textured tapes of $\text{Bi}_2\text{Sr}_2\text{Ca}_2\text{Cu}_3\text{O}_x$ which is estimated as a promising material for technical applications at 77 K. However, problems arise due to severe influence of flux creep at high fields especially for field orientation parallel to the c axis. We address these problems in the present paper by investigations by means of torque magnetometry. This method has been probed to be useful for an elucidation of all kinds of anisotropy, e.g., of the vortex lattice energy (e.g., Refs. 19–21) and vortex pinning.^{21–24} With the torque method one starts relaxation from a steady state. Problems with flux redistribution and overshoot effects which may occur with field sweep methods may be avoided. In the case of torque magnetometry the induction of the sample is nearly constant during the whole cycle of field rotation. Problems with incomplete field penetration are avoided if the magnitude of the rotating field is large enough. Using a very sensitive torquemeter we were able to observe relaxation for several field orientations nearly up to equilibrium. The equilibrium torque value may be determined with the necessary accuracy in order to check quantitatively deviations from a logarithmic decay law. This aspect is ignored in some papers and accordingly strange effects may result. We will show that the measured torque relaxation data may be interpreted by a logarithmic pinning barrier. From relaxation data we derive current-voltage characteristics. It will be shown for the present case of high current density tapes of $\text{Bi}_2\text{Sr}_2\text{Ca}_2\text{Cu}_3\text{O}_x$ that a power law holds over five orders of magnitude of the induced electric field with the power depending in a typical manner on the field component parallel to the c axis.

II. EXPERIMENTAL DETAILS

The present experiments were performed with melt-processed polycrystalline Bi-Sr-Ca-Cu-O in the form of a silver-sheathed tape. The tape was prepared by a special process involving several annealing and pressing steps.²⁵ Resistivity measurements show a transition to the normal state at $T_c = 106$ K with a transition width $\Delta T = 3$ K, re-

vealing that the samples are mainly of the 2:2:2:3 type. Investigations by scanning electron microscopy show that the samples consist of platelike grains. The plate normals which are identical with the c axes are aligned within an angular range of 10° parallel to the tape normal.²⁵ Specimens of 5 mm length with a cross section of the superconducting core of $1.65 \times 0.025 \text{ mm}^2$ were cut from the tape for measurements. The smallest dimension is parallel to the mean c -axis direction.

Torque measurements were performed after zero-field cooling at constant temperature of 77 K as described previously (e.g., Ref. 24). Two types of experiments were carried out. First, an external magnetic field was turned in a plane which contains the mean c -axis direction perpendicular to the tape. The torque G exerted on the sample was measured in dependence on the angle θ between field direction and the mean c -axis direction. Measurements were carried out for field rotation with forward (G_f) and reverse rotational sense (G_r) in order to get information on rotational hysteresis losses. Field rotation rate was 1 deg/s for all experiments with exception of one run where the rate dependence was investigated in the range 1–10 deg/s. From the experimental torque data, reversible (G_{rev}) and irreversible (G_{irr}) torque contributions were determined according to

$$G_{\text{rev}} = \frac{1}{2}(G_f + G_r), \quad (1a)$$

$$G_{\text{irr}} = \frac{1}{2}(G_f - G_r). \quad (1b)$$

In a second group of experiments, the relaxation of the torque after stopping the stationary rotation of the external magnetic field \mathbf{H}_{ext} was measured for several values of H_{ext} and various directions θ . The relaxing torque was recorded for a period of about 10^4 s.

III. EXPERIMENTAL RESULTS

Examples of typical torque curves $G(\theta)$ are shown in Figs. 1(a)–1(c) as dotted lines for several values of the external magnetic field. The angle θ is measured beginning from the c axis as sketched in the inset in Fig. 1(a). The reversible torque contribution determined according to Eq. 1(a) is shown as a solid line in Figs. 1(a)–1(c). Moreover, traces of relaxation experiments are shown as vertical line pieces in Figs. 1(b) and 1(c) which approach the reversible curve. The irreversible torque contributions $G_{\text{irr}}(\theta)$, i.e., the rotational hysteresis losses caused by pinning of the vortices, were extracted from the experimental torque curves according to Eq. (1b). Results are shown in Fig. 2 for several values of the external magnetic field \mathbf{H}_{ext} . With increasing \mathbf{H}_{ext} the irreversible torque becomes more anisotropic. This torque contribution is caused by the pinning of vortices and may be used for estimation of the critical-current density as discussed below.

Relaxation curves $G(t)$ were measured as above described for different stopping angles θ . The approach to equilibrium is demonstrated by the results shown in Fig. 1(c). It may be seen that the relaxation traces from both the forward as well as the reverse curve almost reach the

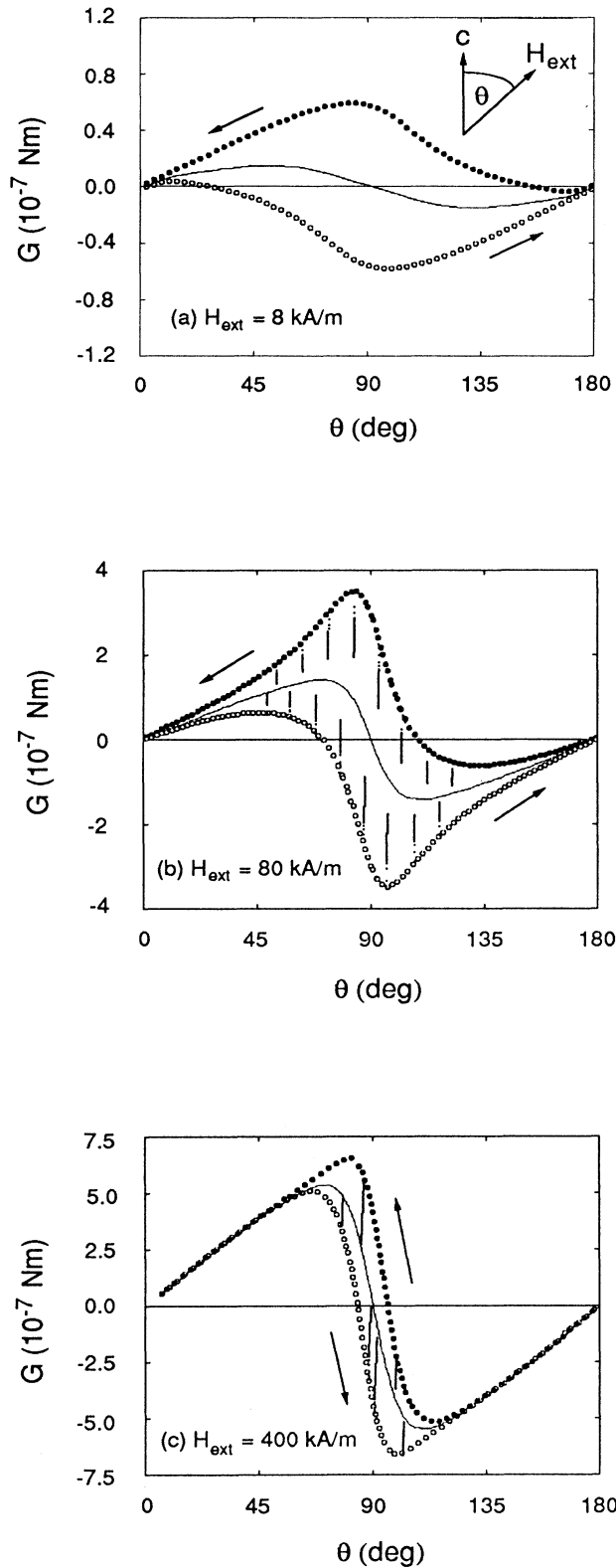


FIG. 1. Dependence of torque on the direction of the external magnetic field (dotted lines), calculated reversible torque (solid line),* and relaxation traces [vertical line pieces in (b) and (c)] for external magnetic fields of (a) 8 kA/m, (b) 80 kA/m, and (c) 400 kA/m.

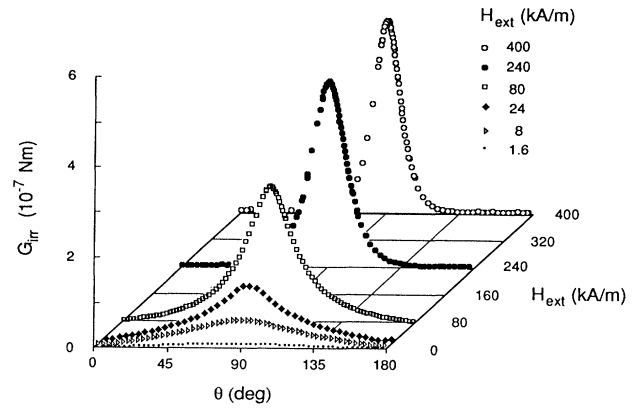


FIG. 2. Dependence of the irreversible torque on the magnitude and orientation of the external magnetic field H_{ext} .

reversible curve. The reversible torque is due to anisotropic contributions to the free energy of the system. It reflects mainly the layered structure of the high- T_c crystal lattice (cf. Ref. 26). For characterization of the relaxation process, we take into account only the irreversible torque part G_{irr} , e.g., the difference between the measured torque $G(t)$ and the value of the reversible torque $G(t_\infty) = G_{\text{rev}}$ determined as described above. Results of relaxation measurements for the case of the external field parallel to the CuO planes as well as under an inclination of $\theta = 45^\circ$ are shown in Fig. 3 with lin-log scaling of the coordinate axes. For the sake of comparison, we have normalized the torque relaxation data with respect to the torque $G(t_0)$ for $t_0 = 1$ s after a stopping field rotation. Relaxation proceeds more rapid for smaller θ and higher values of the external field. One may see that the often used lin-log plot gives curved lines especially for the case of higher fields for which the relaxation proceeds rapidly. Only for the case that the relaxing quantity is yet far from equilibrium may the relaxation be approximated by a logarithmic dependence. The data evaluation performed below shows that the relaxation process obeys a power law in the whole investigated range.

IV. DISCUSSION

A. Anisotropy of losses

The measured torque is given by

$$G/V = \mu_0 \mathbf{M} \times \mathbf{H}_{\text{ext}}, \quad G/V = \mu_0 M H_{\text{ext}} \sin(\mathbf{M}, \mathbf{H}_{\text{ext}}), \quad (2)$$

where V is the sample volume, \mathbf{H}_{ext} is the external magnetic field, and \mathbf{M} is the magnetization of the superconductor related to the flux density \mathbf{B} and the internal field \mathbf{H}_{int} by $\mathbf{M} = \mathbf{B}/\mu_0 - \mathbf{H}_{\text{int}}$. The magnetization may be split into a reversible part \mathbf{M}_{rev} and an irreversible part \mathbf{M}_{irr} . The reversible one is a function of the field direction due to the anisotropy of the system free energy (cf., e.g., Ref. 26). In the present case of textured material, the intrinsic anisotropy of the layered superconductor is masked by the broadening effect of the orientation distribution function of the grain ensemble. For that reason an analysis of

those curves with respect to the anisotropy ratio of the effective electron masses is beyond the scope of the present paper.

The irreversible part of the magnetization, \mathbf{M}_{irr} , occurs in the case of torque magnetometry due to the steady change of the field orientation which forces the vortex system in a nonequilibrium configuration. The irreversible part of the magnetic moment, \mathbf{m}_{irr} , is related to the current density \mathbf{J} in the sample according to

$$\mathbf{m}_{\text{irr}} = \frac{1}{2} \int \mathbf{r} \times \mathbf{J} d^3r. \quad (3)$$

The current density is related in a nonlinear, tensorial way to the electrical field \mathbf{E} , which is induced by the changing induction \mathbf{B} in the sample. The problem of finding the J - E relations will be dealt with in Sec. IV C. A complete theoretical analysis of that problem was given by Klupsch²⁷ for a disklike sample, for which the current is confined to the disk plane; i.e., \mathbf{M} has only a component M_z parallel to the disk normal. In that case one may calculate critical-current densities²⁸ from torque results in analogy to the well-known Bean model. In this way, for instance, the orientation dependence of large ir-

reversible torque for c -axis textured Y-Ba-Cu-O films may be understood.²⁴ The following experimental arguments show that the magnetization in the present case of Bi-Sr-Ca-Cu-O has merely a z component which depends on the z component of the external magnetic field, only. The experimental torque curves of Fig. 1 show that for a field parallel to the c axis ($\theta=0^\circ$) there is no transverse component of the magnetization which would involve currents flowing perpendicular to the CuO planes. We derive the value of the irreversible magnetization M_{irr} from the irreversible torque contribution (Fig. 2) by using Eq. (2) and assuming $\sin(\mathbf{M}, \mathbf{H}_{\text{ext}}) = \sin\theta$:

$$M_{\text{irr}} = G_{\text{irr}} / (V\mu_0 H_{\text{ext}} \sin\theta). \quad (4)$$

Then we get the curves shown in Fig. 4. Plotting that data versus $H_z = H_{\text{ext}} \cos\theta$, we get a single curve shown in Fig. 5. There, regarding the texture width, we took into account the misorientation of grains by assuming for the case of a field perpendicular to the texture axis a value $\theta=85^\circ$. From the irreversible magnetization, one may calculate a critical-current density according to an extension of the Bean model to the present case of a turning field.²⁸ We have provided in Fig. 5 a second scale on the right-hand side of the figure showing critical-current densities estimated according to $J_c = 4M_{\text{irr}}/D$ (D is the sample width).²⁹ In this way the figure demonstrates the strong dependence of critical currents on the field component H_z parallel to the c axis. With increase of that field component, the critical-current density decreases nearly exponentially. A nearly exponential decay of critical currents with increasing field was reported also for Y-Ba-Cu-O (e.g., Refs. 30 and 31). However, because of

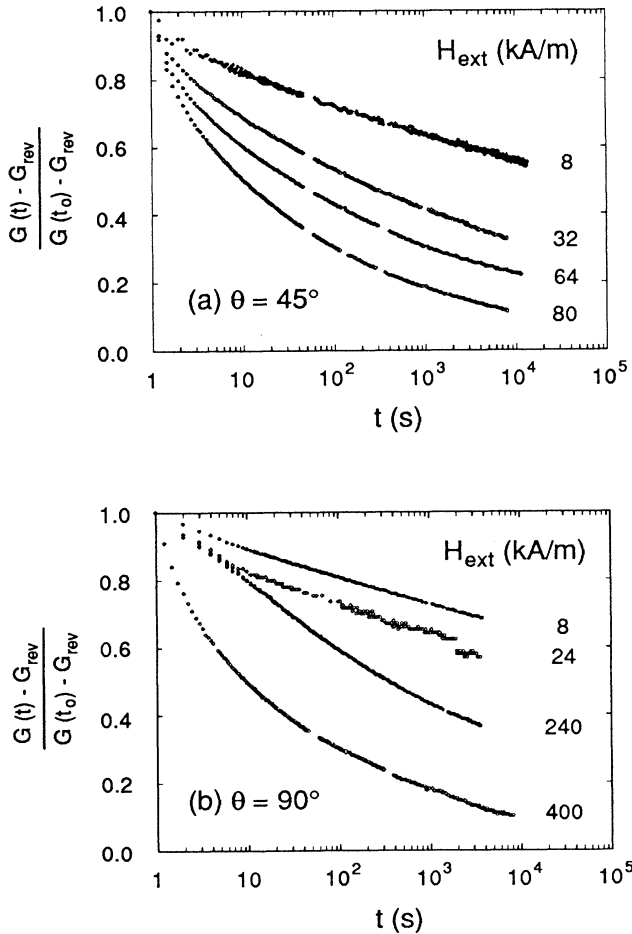


FIG. 3. Relaxation of the torque in different external magnetic fields for directions (a) $\theta=45^\circ$ and (b) $\theta=90^\circ$ (i.e., parallel to the mean orientation of the CuO planes).

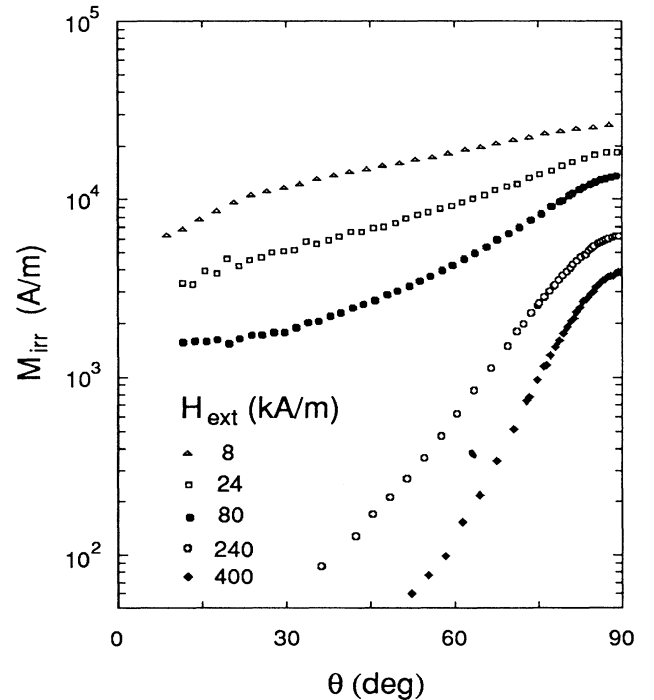


FIG. 4. Irreversible magnetization in dependence on the direction θ for different values of the magnetic field.

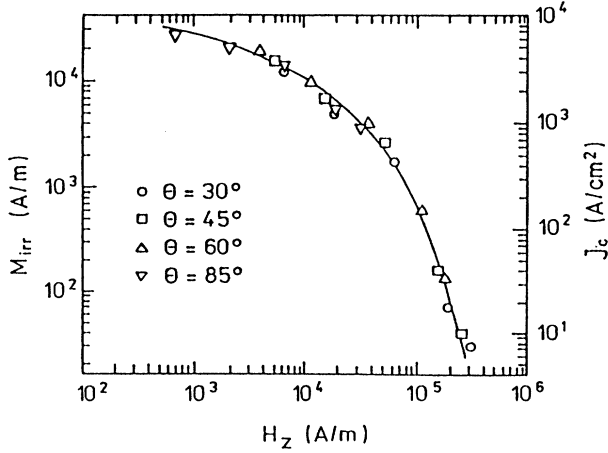


FIG. 5. Irreversible magnetization (left scale) and critical-current density (right scale) vs the field component H_z parallel to the c axis.

the dependence of J_c only on the component H_z in the present Bi-Sr-Ca-Cu-O material, one may expect for the ideal parallel-field configuration (i.e., a sample with ideal alignment of the ab planes and the field) critical-current densities independent of the field amplitude as high as the zero-field value. The excellent scaling of M_{irr} with the field component H_z independent of the angle θ confirms the assumption that \mathbf{M}_{irr} is aligned with the c axis during the whole cycle of field rotation. Accordingly, the associated currents are confined to the ab plane. The torque data reflect the typical anisotropy of dissipation in layered high- T_c materials, which was also found by angular-dependent electrical-transport measurements.^{18,32,33} Scaling of the magnetic response with the field component parallel to the c axis was found also by Duran *et al.*³⁴ by ac-susceptibility measurements on Bi-Sr-Ca-Cu-O. Taking into account a typical demagnetization factor $N_{zz}=0.97$ for the present samples, one can see that in the whole parameter range of our measurements $\mu_0 H_z$ is nearly identical with the flux density B_z . Obviously, dissipation may be understood as due to motion of pancake vortices which are driven during field rotation along the CuO planes, thereby surmounting pinning barriers due to crystal defects located in the CuO planes. This picture was already used by Kes *et al.*³⁵ for explaining several experimental results for the case of a field parallel to the CuO planes. The kind of defects responsible for pinning of pancake vortices is not yet clear. Tachiki, Koyama, and Takahashi³⁶ have suggested a model for explaining the experimentally found critical-current anisotropy³² by assuming that vortex kinks are pinned by some kind of planar defects perpendicular to the CuO planes. We have shown recently²² that planar defects (e.g., twin planes in Y-Ba-Cu-O) have no influence on the maximum of the irreversible torque component which arises for the field direction parallel to the CuO planes. Moreover, in the present samples planar defects parallel to the c axes of the grains may not be expected. Instead, point defects (e.g., oxygen vacancies) in CuO planes may represent pinning centers for point vortices as

was argued previously by Kes *et al.* (e.g., Ref. 35).

The observed H_z dependence of the irreversible magnetization (Fig. 5) shows that pinning decreases remarkably with increasing field component parallel to the c axis; regardless, the field amplitude is raised or the field orientation is changed toward the c -axis direction ($\theta=0^\circ$). Both latter processes are associated with an increase of pancake density and a related increase of pancake interaction. On the contrary, when the field direction approaches the CuO planes ($\theta=90^\circ$), the pancake lattice becomes extremely diluted and interactions fade away. With decreasing field amplitude, vortex interaction decreases too and the apparent anisotropy of the irreversible magnetization vanishes (cf. Fig. 4). This picture is confirmed by the second group of experiments discussed in the next section, which deals with torque relaxation.

In the case of Y-Ba-Cu-O, deviations from the just discussed model of the quasi-two-dimensional layered superconductor are observed. Fischer *et al.*³⁷ have reported magnetization measurements on single crystals of Y-Ba-Cu-O for several field directions. Their results show that only in a range $0^\circ \leq \theta \leq 60^\circ$ are screening currents nearly confined to the CuO planes.

B. Torque relaxation

The measured torque relaxation data shown in Fig. 3 may be easily transferred into magnetization data using Eq. (4) and taking advantage of the discussion of Sec. IV A. The results are plotted in Fig. 6 in a log-log plot. All curves are rather straight. The slope increases with increasing field. It is obvious that the Anderson-Kim approach cannot explain the data at least for higher field values. We compare our experimental data with relevant models from the literature which are characterized by the assumption of different dependences of the barrier height on current density: the inverse power-law barrier,²⁻⁸ the logarithmic barrier,⁹ and the linear barrier according to Anderson and Kim.¹ The interpolation formula resulting from the vortex-glass^{6,2} or collective-creep model,⁷

$$M(t) = M_0 [1 + pkT/U_0 \ln(t/t_{eff})]^{-1/p} \quad (5)$$

is related to an inverse power-law barrier

$$U(J) = (U_0/p) [(J_0/J)^p - 1], \quad (6)$$

which gives a relaxation rate

$$S = - \frac{d \ln M}{d \ln t} = \frac{kT}{U_0 + pkT \ln(t/t_{eff})}. \quad (7)$$

The logarithmic barrier⁹

$$U(J) = U_0 \ln(J_0/J) \quad (8)$$

leads to a power law

$$M(t) = M_0 (t/t_{eff})^{-S}, \quad (9)$$

with

$$S = kT/U_0. \quad (10)$$

In the Anderson-Kim flux-creep model,¹ one has

$$M(t) = M_0 [1 - kT/U_0 \ln(t/t_{\text{eff}})], \quad (11)$$

$$U(J) = U_0 (1 - J/J_0), \quad (12)$$

$$S = kT / [U_0 - kT \ln(t/t_{\text{eff}})], \quad (13)$$

where U_0 is the undisturbed pinning barrier for current $J=0$ and t_{eff} is a characteristic time depending on microscopic properties and initial conditions. Comparison of the decay functions [Eqs. (5), (9), and (11)] shows that the latter two equations may be regarded as special cases of the interpolation formula Eq. (5). The logarithmic barrier results from the inverse power law in the limit $p \rightarrow 0$. The Anderson-Kim formula represents the case $p = -1$. Further characteristic values of p are derived within the collective-creep model.⁷ At least three creep regimes are distinguished: $p = \frac{1}{7}$ for single-vortex creep, $p = \frac{3}{2}$ for hopping of small bundles with a transverse size $R \ll \lambda$ (λ is the London penetration depth), and $p = \frac{7}{9}$ for hopping of large bundles. For 2D collective creep, a value $p = \frac{9}{8}$ is proposed.³⁸ These exponents were derived for small hopping distances $L \ll a$ (a vortex-lattice constant). In the opposite limit,^{12,39} the value $p = \frac{1}{2}$ may be derived.

In order to check the suitability of the different models

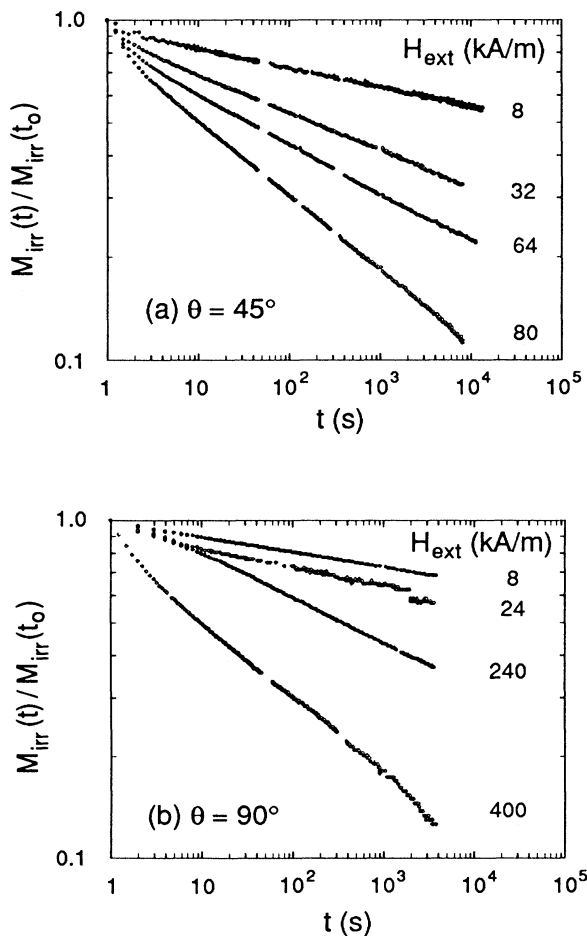


FIG. 6. Relaxation of the irreversible part of the magnetization for different external magnetic fields for directions (a) $\theta=45^\circ$ and (b) $\theta=90^\circ$.

for a description of the present experimental data, we have tried to fit our data using Eq. (5) for several characteristic values of the power p . Results are demonstrated in Fig. 7 for an example of rapid relaxation with a relatively large field inclined by an angle of 45° with respect to the c axis. There, we have plotted the experimental data in a frame $[M/M_0]^{-p}$ versus $\ln(t/t_{\text{eff}})$ for distinct values of p . There, a value of 10^{-3} s was chosen for t_{eff} . Curves of the type given by Eq. (5) are straight lines in the plot of Fig. 7. Apparently, the experimental data lie on curved lines for p values that are different from zero. As a quantitative measure, we have given in the inset of Fig. 7 the goodness Q of fitting with straight lines in dependence on the power p . The best fit [i.e., the maximum of the curve $Q(p)$] is given for a value $p=0.06$, which is closer to $p=0$ than to any other of the above-mentioned theoretical values. This confirms the earlier arguments in favor of a logarithmic barrier.⁹⁻¹³ It should be pointed out that a spurious bending of decay curves may occur at large times due to an error δM_{rev} of the value of the reversible magnetization. The accuracy of the end value of the relaxation $M(t_\infty) = M_{\text{rev}}$ determines the maximum time up to which the error δM_{rev} causes in bi-logarithmic representation of decay curves a spurious curvature either upward if a too small value of M_{rev} is assumed or downward if M_{rev} is overestimated. In the present experiments, the condition $\delta M_{\text{rev}} \ll M_{\text{irr}}(t_{\text{max}})$ is always fulfilled, where $t_{\text{max}} = 10^4$ s is the maximum

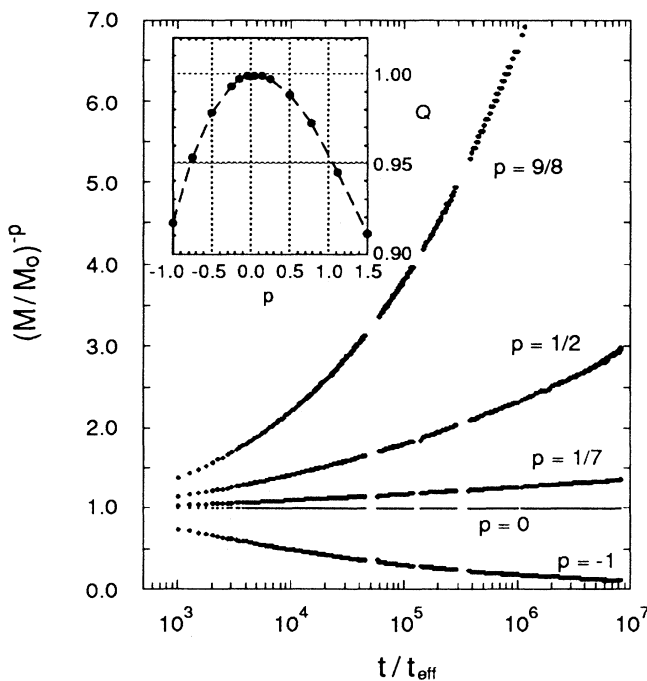


FIG. 7. Experimental decay data ($H_{\text{ext}}=80$ kA/m, $\theta=45^\circ$) in a M^{-p} vs $\ln t$ plot for different p values: $p = \frac{1}{7}$, $\frac{1}{2}$, and $\frac{9}{8}$ (interpolation formula [Eq. (5)]); $p=0$ (power law [Eq. (9)]); $p=-1$ (Anderson-Kim [Eq. (11)]). In the inset the correlation coefficient Q for a fit of the experimental data with Eq. (5) is given as dependent on p .

measuring time. We can clearly rule out for our data the exponents $p = \frac{3}{2}$ and $\frac{7}{9}$ predicted for the low-current regime of the collective-creep model (hopping of vortex bundles). Also, the value $p = \frac{9}{8}$ given for 2D creep as well as the value $p = \frac{1}{2}$ cannot be confirmed by our results. Regarding the high temperature and the very low current densities of the present results, single-vortex creep—characterized in the collective-creep model by a value $p = \frac{1}{7}$ —seems to be unlikely. Comparing experimental values of p reported in the literature, one observes a considerable scattering of the data. For the case of Y-Ba-Cu-O, besides logarithmic decay ($p = -1$) there are given small values of $0.1 \leq p \leq 0.5$ (Ref. 40) or even zero (logarithmic barrier)^{9,10} as well as values up to $p = 3$.⁵ Thompson, Sun, and Holtzberg³ have reported the temperature dependence of p for the range $4.2 \leq T \leq 70$ K. They found a maximum of p at $T = 30$ K with roughly $p = \frac{3}{2}$. Remarkably, the decrease of p at higher T may be extrapolated to $p = 0$ at about 80 K. For the case of $\text{Bi}_2\text{Sr}_2\text{CaCu}_2\text{O}_x$, Svedlind *et al.*¹⁶ fit their data by $\ln(t/t_0)^{-p}$, which differs from the interpolation formula at least by a factor of p^{-1} . They report $1.0 < p < 1.8$ and $10^{-5} < t_{\text{eff}} < 10^{-3}$ s. van der Beek *et al.*¹⁷ report for $\text{Bi}_2\text{Sr}_2\text{CaCu}_2\text{O}_{8+x}$ single crystals a $U(J)$ dependence at high current densities close to logarithmic. However, for fitting the same data by $U_c(J_c/J)^p$, they claim a crossover from $p = \frac{9}{8}$ at high currents to $p = \frac{1}{2}$ at lower ones. The reason for the inconsistency of most literature data is not yet clear as was pointed out in Ref. 40 too. The present investigations on $\text{Bi}_2\text{Sr}_2\text{Ca}_2\text{Cu}_3\text{O}_x$ tapes differ from the literature data besides by the material and experimental procedures and also by the temperature and field range. Present data refer to a comparatively high temperature of 77 K, where one deals with a regime of very rapid relaxation near the irreversibility line or—in the framework of the vortex-glass model—with the critical region near the vortex-glass transition. Comparing with Y-Ba-Cu-O data, one should regard that in the present case of Bi-Sr-Ca-Cu-O we deal with a much more anisotropic material, the quasi-two-dimensional character of which makes the predictions of the vortex-glass model questionable. It should be pointed out that the present data are the closest to the irreversibility line available in the literature until now. So differences of p values to the literature data may not be surprising. Moreover, we argue that the power-law decay ($p = 0$) reported here may be typical for the close neighborhood of the irreversibility line.

C. Electrical-field–current-density characteristics

Above, we have given arguments that the irreversible part of the magnetization has only a z component parallel to the c axis. Consequently, only a component J parallel to the CuO planes occurs. Then we may calculate the current density according to $J(t) = 4M_{\text{irr}}(t)/D$ (D is the sample width).²⁹ The electric field may be calculated according to

$$\nabla \times \mathbf{E} = - \frac{d\mathbf{B}}{dt},$$

which may be approximated by

$$E = \frac{D}{2} \mu_0 \left[\frac{dH_z}{dt} + \frac{dM_z}{dt} \right] \quad (14)$$

(sample width D), where M_z is determined by Eq. (4) and a minor change of $H_z = H \cos\theta$ is taken into account, which arises in our noncompensated torquemeter due to a very small change of the sample orientation during torque relaxation. In this way we have calculated from the relaxation curves $G(t)$ the dependence of the electrical field on the current density. Results of the calculations are shown in Fig. 8. They demonstrate the validity of a power law for the electric-field–current-density characteristic. A consequence of a power law is an ambiguity of the definition of “critical”-current densities. Discrepancies in the literature regarding J_c values determined by electrical and magnetic methods (e.g., Refs. 24 and 30) may be caused by using different voltage criteria for defining critical-current densities J_c on the nonlinear current-voltage characteristics. Comparing results of both methods, Ries, Neumüller, and Schmidt²⁹ found for melt-processed $\text{Bi}_2\text{Sr}_2\text{CaCu}_2\text{O}_x$ a power law too. At lower temperatures, Kim *et al.*⁴¹ found a negative curvature in a log-log plot of current-voltage characteristics which allows a reasonable definition of J_c . The transition to power-law behavior in the current-voltage characteristics was interpreted by Koch *et al.*⁴² as the vortex-glass transition temperature.

According to the work of Zeldov *et al.*,⁹ a logarithmic barrier leads to a power law for the E - J dependence,

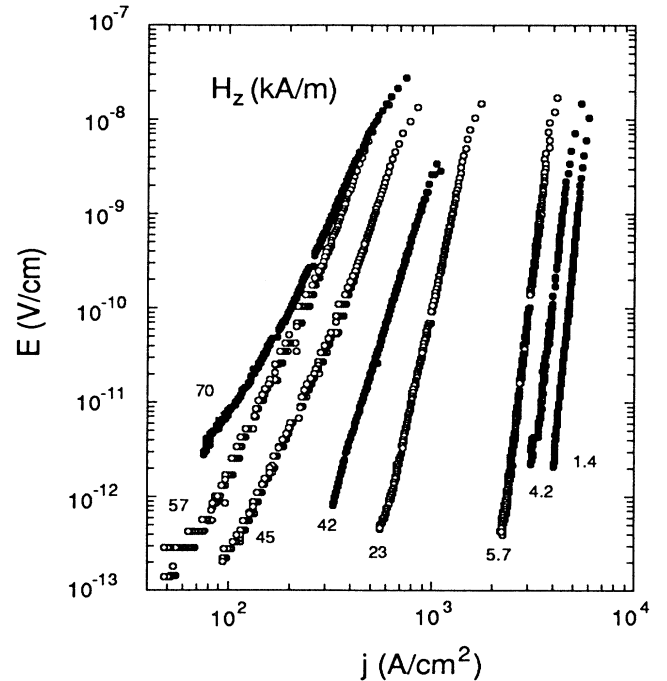


FIG. 8. Electrical-field–current-density characteristics derived from torque relaxation for $\theta = 45^\circ$ (\circ) and $\theta = 90^\circ$ (\bullet) for different values of H_z .

$$E/E_0 = (J/J_0)^{U_0/kT}, \quad E_0 = v_0 L B, \quad (15)$$

where v_0 is an attempt frequency and L a hopping distance. We have combined in Fig. 8 data of measurements for different orientation and amplitude of the external magnetic field with the corresponding z component of the field given on each curve. There, we have taken into account the grain misorientation by assuming a value $\theta=80^\circ$ for the case of a field parallel to the tape plane. The results show that the slope U_0/kT of the $E(J)$ curves is determined by H_z independently of the field direction and field magnitude. For comparison, we have performed electrical-transport measurements for samples manufactured by the same process. The data cover a range of the electric field of $(0.5-1.7) \times 10^{-6}$ V/cm. In comparison, electrical-field values realized by torque magnetometry are at least two orders of magnitude smaller. Electrical measurements were performed for two directions of the magnetic field: parallel to the c axis ($\theta=0^\circ$) and at an angle $\theta=90^\circ$. Note that the case $\theta=0^\circ$ is not accessible for torque magnetometry. The data also obey a power law and scale with the field component H_z . The pinning barrier U_0/kT determined from the power of the $E-J$ curves is plotted in Fig. 9 in dependence on the field component H_z for the magnetic as well as the electrical measurement data. There is a remarkable match of all data obtained by electrical as well as magnetic methods with different magnetic-field magnitudes of 1.6–2000 kA/m. It should be noted that the data comprise different field directions θ . Here, again, we see the scaling of the data with $H_z = H_{\text{ext}} \cos\theta$. The coincidence of the data for the different field directions on one curve shows that the relaxation rate is determined by the pancake density in such a way that U_0 decreases with increasing flux density. The data show roughly a dependence H_z^{-n} , where n varies from $\frac{1}{3}$ at low H_z to nearly 1 at the highest pancake densities. In the literature, $n=1$ was suggested (e.g., Ref. 43). However, experimental data in the literature scatter considerably. Comparing the data with the relaxation curves of Fig. 3, one may see that especially those curves deviate from logarithmic behavior according to Anderson and Kim which are characterized by low U_0/kT . For a maximum observation time of about 10^4 s in the present measurements, deviations from logarithmic creep become apparent for $U_0/kT < 10$. In that case of “rapid” relaxation, we deal in the neighborhood of the so-called irreversibility line.

V. CONCLUSIONS

We have investigated the layered superconductor $\text{Bi}_2\text{Sr}_2\text{Ca}_2\text{Cu}_3\text{O}_x$ by torque magnetometry with respect to the anisotropy of dissipation effects due to vortex motion. It was shown that the influence of both the field magni-

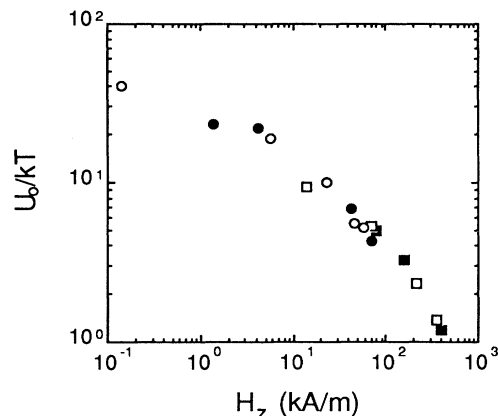


FIG. 9. Dependence of the relative barrier height U_0/kT on the field component c parallel for torque magnetometry [$\theta=45^\circ$ (\bullet), $\theta=90^\circ$ (\circ)] and electrical transport [$\theta=0^\circ$ (\blacksquare), $\theta=90^\circ$ (\square)].

tude as well as the field direction may be reduced to the dependence on the field component parallel to the c axis, which represents the density of pancake vortices situated on CuO planes. Losses (e.g., rotational hysteretic ones) arise when the pancake vortices are forced by a change of the external magnetic field to move along the CuO planes. Thereby, they experience the pinning potential of defects situated in those planes. The resulting pinning barrier decreases strongly with increasing vortex density. Torque relaxation results show that the flux-creep model of Anderson and Kim¹ is applicable only in a parameter range where creep effects are small. Otherwise, decay curves follow a power law which is in accordance with a logarithmic pinning barrier suggested previously by Zeldov *et al.*⁹ for Y-Ba-Cu-O thin films. The logarithmic barrier differs from other suggestions in the literature regarding the shape in real space of pinning potentials $U(x)$ by its long-range tail. A physical justification of that potential shape was already given by Zeldov *et al.*⁹ The somewhat exotic behavior of that potential for $x \rightarrow 0$ may be eliminated by a correction according to a suggestion by Welch.⁴⁴ Our experimental data suggest that the pinning of pancake vortices in extremely layered CuO-based materials in the vicinity of the irreversibility line may be described by a logarithmic barrier.

ACKNOWLEDGMENTS

The authors thank Professor W. Andrä, Dr. T. Klupsch, and Dr. H. Pfeiffer for valuable discussions as well as Dr. W. Wilhelm for sample preparation. This work was supported by the Bundesministerium für Forschung und Technologie under Contract No. 13.N.5928.

¹P. W. Anderson and Y. B. Kim, *Rev. Mod. Phys.* **36**, 39 (1964).

²A. P. Malozemoff and M. P. A. Fisher, *Phys. Rev. B* **42**, 6784 (1991).

³J. R. Thompson, Y. R. Sun, and F. Holtzberg, *Phys. Rev. B* **44**,

458 (1991).

⁴M. Konczykowski, A. P. Malozemoff, and F. Holtzberg, *Physica C* **185-189**, 2203 (1991).

⁵E. Sandvold and C. Rossel, *Physica C* **190**, 309 (1992).

- ⁶M. P. A. Fisher, *Phys. Rev. Lett.* **62**, 1415 (1989).
- ⁷M. V. Feigelman and V. M. Vinokur, *Phys. Rev. B* **41**, 8986 (1990).
- ⁸A. P. Malozemoff, *Physica C* **185-189**, 264 (1991).
- ⁹E. Zeldov, M. M. Amer, G. Koren, A. Gupta, M. W. McElfresh, and R. J. Gambino, *Appl. Phys. Lett.* **56**, 680 (1990).
- ¹⁰M. P. Maley and J. O. Willis, *Phys. Rev. B* **42**, 2639 (1990).
- ¹¹M. E. McHenry, S. Simizu, H. Lessure, M. P. Maley, J. Y. Coulter, I. Tanaka, and H. Kojima, *Phys. Rev. B* **44**, 7614 (1991).
- ¹²V. V. Vinokur, G. Blatter, M. Feigelman, V. B. Geshkenbein, and A. Larkin, *Physica C* **185-189**, 276 (1991).
- ¹³V. V. Vinokur, M. Feigelman, and V. B. Geshkenbein, *Phys. Rev. Lett.* **67**, 915 (1991).
- ¹⁴C. W. Hagen and R. Griessen, *Phys. Rev. Lett.* **62**, 2875 (1989).
- ¹⁵D. Shi and M. Xu, *Phys. Rev. B* **44**, 4548 (1991).
- ¹⁶P. Svedlindh, C. Rossel, K. Niskanen, P. Norling, P. Nordblad, L. Lundgren, and G. V. Chandrashekar, *Physica C* **176**, 336 (1991).
- ¹⁷C. J. van der Beek, P. H. Kes, M. P. Maley, M. J. V. Menken, and A. A. Menovsky, *Physica C* **185-189**, 2507 (1991).
- ¹⁸M. P. Maley, P. J. Kung, J. Y. Coulter, W. L. Carter, G. N. Riley, and M. E. McHenry, *Phys. Rev. B* **45**, 7566 (1992).
- ¹⁹D. E. Farrell, S. Bonham, J. Foster, Y. C. Chang, P. Z. Jiang, K. G. Vandervoort, D. J. Lam, and V. G. Kogan, *Phys. Rev. Lett.* **63**, 782 (1989).
- ²⁰K. E. Gray, R. T. Kampwirth, and D. E. Farrell, *Phys. Rev. B* **41**, 819 (1990).
- ²¹B. Janossy, R. Hergt, and L. Fruchter, *Physica C* **170**, 22 (1990).
- ²²R. Hergt, W. Andrä, R. Hiergeist, and J. Taubert, *Phys. Status Solidi A* **129**, 237 (1992).
- ²³L. Fruchter, C. Aguillon, I. A. Campbell, and B. Keszei, *Phys. Rev. B* **42**, 2627 (1990).
- ²⁴W. Andrä, H. Bruchlos, T. Eick, R. Hergt, W. Michalke, W. Schüppel, and K. Steenbeck, *Physica C* **180** 184 (1991).
- ²⁵M. Wilhelm, H. W. Neumüller, and G. Ries, *Physica C* **185-189**, 2399 (1991).
- ²⁶Z. Hao and J. R. Clem, *Phys. Rev. B* **43**, 7622 (1992).
- ²⁷T. Klupsch, *Physica C* **197**, 241 (1992).
- ²⁸C. W. Hagen, M. R. Bom, R. Griessen, B. Dam, and H. Veringa, *Physica C* **153-155**, 322 (1988).
- ²⁹G. Ries, H. W. Neumüller, and W. Schmidt, *Supercond. Sci. Technol.* **5**, S81 (1992).
- ³⁰P. Fischer, H. W. Nuemüller, B. Roas, H. F. Braun, and G. Saemann-Ischenko, *Solid State Commun.* **72**, 871 (1989).
- ³¹S. Senoussi, M. Oussena, G. Collin, and I. A. Campbell, *Phys. Rev. B* **37**, 9792 (1988).
- ³²Y. Iye, A. Fukushima, T. Tamegai, T. Terashima, and Y. Bando, *Physica C* **185-189**, 297 (1991).
- ³³H. Raffi, S. Labdi, O. Laborde, and P. Monceau, *Phys. Rev. Lett.* **66**, 2515 (1991).
- ³⁴C. Duran, J. Yazzi, F. de la Cruz, D. J. Bishop, D. B. Mitzi, and A. Kapitulnik, *Phys. Rev. B* **44**, 7737 (1991).
- ³⁵P. H. Kes, J. Aarts, V. M. Vinokur, and C. J. van der Beek, *Phys. Rev. Lett.* **64**, 1063 (1990).
- ³⁶M. Tachiki, T. Koyama, and S. Takahashi, *Physica C* **185-189**, 303 (1991).
- ³⁷P. Fischer, R. Busch, H. W. Neumüller, G. Ries, and H. F. Braun, *Supercond. Sci. Technol.* **5**, S440 (1992).
- ³⁸V. M. Vinokur, P. H. Kes, and A. E. Koshelev, *Physica C* **168**, 29 (1990).
- ³⁹T. Natterman, *Phys. Rev. Lett.* **64**, 2454 (1990).
- ⁴⁰Y. Ren and P. A. J. de Groot, *Physica C* **196**, 111 (1992).
- ⁴¹D. H. Kim, K. A. Gray, R. T. Kampwirth, and D. M. McKay, *Phys. Rev. B* **42**, 6249 (1990).
- ⁴²R. H. Koch, V. Foglietti, W. J. Gallagher, G. Koren, A. Gupta, and M. P. A. Fisher, *Phys. Rev. Lett.* **63**, 1511 (1989).
- ⁴³M. Tinkham, *Phys. Rev. Lett.* **61**, 1658 (1988).
- ⁴⁴D. C. Welch, *IEEE Trans. Magn.* **27**, 1133 (1991).